

# How native state topology affects the folding of Dihydrofolate Reductase and Interleukin-1 $\beta$

Cecilia Clementi<sup>1</sup>, Patricia A. Jennings<sup>2</sup>, José N. Onuchic<sup>1</sup>  
*Department of Physics<sup>1</sup> and Department of Chemistry and Biochemistry<sup>2</sup>*  
*University of California at San Diego La Jolla, California 92093, USA*

The overall structure of the transition state and intermediate ensembles experimentally observed for *Dihydrofolate Reductase* and *Interleukin-1 $\beta$*  can be obtained utilizing simplified models which have almost no energetic frustration. The predictive power of these models suggest that, even for these very large proteins with completely different folding mechanisms and functions, real protein sequences are sufficiently well designed and much of the structural heterogeneity observed in the intermediates and the transition state ensembles is determined by topological effects.

## I. INTRODUCTION

Explaining how proteins self-assemble into well defined structures is a longstanding challenge. Energy landscape theory and the funnel concept (1–7) have provided the theoretical framework necessary for improving our understanding of this problem — efficient folding sequences minimize frustration. Frustration may arise from the inability to satisfy all native interactions and from strong non-native contacts which can create conformational traps. The difficulty of minimizing energetic frustration by sequence design, however, is also dependent on the choice of folding motif. Some folding motifs are easier to design than others (8,9), suggesting the possibility that evolution not only selected sequences with sufficiently small energetic frustration but also selected more easily designable native structures. To address this difference in foldability, we have introduced the concept of “topological frustration” (10–13) — even when sequences have been designed with minimal energetic frustration, variations in the degree of nativeness of contacts in the transition state ensemble (TSE) are observed because of asymmetries imposed by the chosen final structure.

Recent theoretical and experimental evidences suggest that proteins, especially small fast folding (sub-millisecond) proteins, have sequences with a sufficiently reduced level of energetic frustration that the global characteristics of the observed heterogeneity observed in the TSE are strongly influenced by the native state topology. We have shown (13) that the overall structure of the TSE for *Chymotrypsin Inhibitor 2* (CI2) and for the SH3 domain of the *src tyrosine-protein kinase* can be obtained by using simplified models constructed by using sequences that have almost no energetic frustration (Gō-like potentials). These models drastically reduce the energetic frustration and energetic heterogeneity for native contacts, leaving the topology as the primary source of the residual frustration. Topological effects, however, go beyond affecting the structure of the TSE. The overall structure of the populated intermediate state ensembles during the folding of proteins such as *Barnase*, *Ribonuclease H* and *CheY* have also been successfully determined using a similar model (13). It is interesting to notice that although these model, since they consider totally unfrustrated sequences, may not reproduce the precise energetics of the real proteins, such as the value of the barrier heights and the stability of the intermediates, they are able to determine the general structure of these ensembles. Therefore, the fact that these almost energetically unfrustrated models reproduce most of the major features of the TSE of these proteins indicate that real protein sequences are sufficiently well designed (i.e. with reduced energetic frustration) that much of the heterogeneity observed in the TSE’s and intermediates have a strong topological dependence.

Do these conclusions hold to larger and slower folding proteins with a more complex folding kinetics than

two-state folders as CI2 and SH3? The success obtained with *Barnase*, *Ribonuclease H* and *CheY* intermediates already provides some encouragement — topology appears to be important in determining on-pathway folding intermediates. In this paper this approach is extended to a pair of larger proteins: *Dihydrofolate Reductase* (DHFR) and *Interleukin-1 $\beta$*  (IL-1 $\beta$ ). The synoptic analysis of these two proteins is particularly interesting because they have a comparable size (slightly over 150 amino-acids), but different native structures, folding mechanisms and functions: DHFR is a two-domain  $\alpha/\beta$  enzyme that maintains pools of tetrahydrofolate used in nucleotide metabolism while IL-1 $\beta$  is a single domain all  $\beta$  cytokine with no catalytic activity on its own but elicits a biological response by binding to its receptor.

## II. NUMERICAL PROCEDURES

The energetically unfrustrated model of DHFR and IL-1 $\beta$  are constructed by using a Gō-like Hamiltonian (14,15). A Gō-like potential takes into account only native interactions, and each of these interactions enters in the energy balance with the same weight. Residues in the proteins are represented as single beads centered in their C- $\alpha$  positions. Adjacent beads are strung together into a polymer chain by means of bond and angle interactions, while the geometry of the native state is encoded in the dihedral angle potential and a non-local bead-bead potential.

A detailed description of this energy function can be found elsewhere (13). The local (torsion) and non-local terms have been adjusted so that the stabilization energy residing in the tertiary contacts is approximately twice as large as the torsional contribution. This balance among the energy terms is optimal for the folding of our Gō-like protein models (4). Solvent mediation and side chain effects are already included in these effective energy functions. Therefore, entropy changes are associated to the configurational entropy of the chain. The native contact map of a protein is derived with the CSU software, based upon the approach developed in ref. (16). Native contacts between pairs of residues ( $i, j$ ) with  $j \leq i + 4$  are discarded from the native map as any three and four subsequent residues are already interacting in the angle and dihedral terms. A contact between two residues ( $i, j$ ) is considered formed if the distance between the C $\alpha$ s is shorter than  $\gamma$  times their native distance  $\sigma_{ij}$ . It has been shown (11) that the results are not strongly dependent on the choice made for the cut-off distance  $\gamma$ . In this work we used  $\gamma = 1.2$ .

For both (DHFR and IL-1 $\beta$ ) protein models, folding and unfolding simulations have been performed at several temperatures around the folding temperature. The results from the different simulations have been combined using the WHAM algorithm (17). Several very different initial unfolded structures for the folding simu-

lations have been selected and they have been obtained from high temperature unfolding simulations. In order to have appropriate statistics, we made sure that for every transition state ensemble or intermediate, we have sampled about 500 uncorrelated conformations (thermally weighted). For smaller proteins such as SH3 and CI2 (that have about 1/3 of the tertiary contacts of DHFR and IL-1 $\beta$ ) we have determined that about 200 uncorrelated conformations in the transition state ensemble are necessary to have an error on the estimates of contact probabilities (or  $\Phi$  values) of  $\pm 0.05$  (13).

### III. COMPARING SIMULATIONS AND EXPERIMENTS FOR DIHYDROFOLATE REDUCTASE AND INTERLEUKIN-1 $\beta$

*Dihydrofolate Reductase* and *Interleukin-1 $\beta$*  not only have dissimilar native folds<sup>1</sup> but also the nature of the intermediate states populated during the folding event is remarkably different. To explore the connection between the protein topology and the nature of the intermediates, we used an energetically minimally frustrated  $C_\alpha$  model for these two proteins, with a potential energy function defined by considering only the native local and non-local interactions as being attractive (see Numerical Procedures, for details). This is a very simplified potential that retains only information about the native fold — energetic frustration is almost fully removed. Notice that although the real amino-acid sequence is not included in this model, the chosen potential is like a “perfect” sequence for the target structure, without the energetic frustration of real sequences (since this potential includes attractive native tertiary contacts, it implicitly incorporates hydrophobic interactions). Therefore, this model provide us with the perfect computational tool to investigate how much of the structural heterogeneity observed during folding mechanism could be inferred from the knowledge of the native structure alone without contributions from energetic frustration.

Since early work suggests that proteins (at least small fast folding proteins) have sufficiently reduced energetic frustration, they have a funnel-like energy landscape with a solvent-averaged potential strongly correlated with the degree of nativeness (but with some roughness due to the residual frustration). In this situation, the folding dynamics can be described as the diffusion of an ensemble of protein configurations over a low dimensional free energy surface — defined in terms of the reaction coordinate

$Q$ , where  $Q$  represents the fraction of the native contact formed in a conformation ( $Q = 0$  at the fully unfolded state and  $Q = 1$  at the folded state) (10–13,18). The ensemble of intermediates observed in this free energy profile are expected to mimic the real kinetic intermediates.

Fig. 1 shows a comparison between the folding mechanism obtained from our simulations for the minimally-frustrated analogue of DHFR (panels (a) and (c)) and IL-1 $\beta$  (panels (b) and (d)). The different nature of the folding intermediates of the two proteins and their native ensembles emerging from these data is in substantial agreement with the experimental observations, with the adenine binding domain of DHFR being folded in the main intermediate in the simulation and the central  $\beta$  strands of IL-1 $\beta$  being formed early in this single domain protein. The absolute values of the free energy barriers resulting from simulations may not necessarily agree with the experimental ones because we are dealing with unfrustrated designed sequences. Thus, quantitative predictions that depend on barrier heights and stability of the intermediate ensembles (e.g. folding time, rate determining barriers and lifetime of intermediates) are not possible for this kind of models. However we show that topology is sufficient to correctly detect the positions of the transition state and intermediate states. A more detailed description follows.

#### A. Dihydrofolate Reductase

The folding process emerging from the dynamics of the G $\phi$ -like analogue of DHFR (as summarized in Fig. 1 (a) and (c)) is interestingly peculiar and consistent with the experimentally proposed folding mechanism (19) (see Fig. 3 (d)). Refolding initiates by a barrierless collapse to a quasi-stable species ( $Q=0.2$ ) which corresponds to the formation of a burst-phase intermediate,  $I_{BP}$ , with little stability but some protection from  $H$ -exchange across the central  $\beta$  sheet (20). This initial collapse is followed by production of the main intermediate  $I_{HF}$  (*Highly Fluorescent*), which is described in the mechanism of Fig. 3 (d) as the collection of intermediates  $I_1 - I_4$ .  $I_1 - I_4$  are structurally similar to each other, but differentiated experimentally by the rate at which they proceed towards the native protein. Finally, after the overcoming of a second barrier, the protein visits an ensemble of native structures with different energies. The experimentally determined folding mechanism of DHFR shows transient kinetic control in the formation of native conformers ( $N_4$  dominant). This is later overridden by thermodynamic considerations ( $N_2$  dominant) at final equilibrium (19). This latter finding is consistent with the nature of the folding ensemble determined by the simulations. As shown in Fig. 3 (b) a set of structures close to the native state ( $Q$  around 0.7-0.8) is transiently populated beside the fully folded state ( $Q = 1$ ). Since

<sup>1</sup>The 162 residues of DHFR arrange themselves in 8  $\beta$ -strands and 4  $\alpha$ -helices, grouped together in the folded state in as detailed in Fig.2 (d), while IL-1 $\beta$  is a 153 residues, all- $\beta$  protein, composed by 12  $\beta$  strands packed together as shown in Fig.4 (c)-(d).

the main intermediate  $I_{HF}$  has been recently characterized by experimental studies (19–24), we take our analysis a step farther by comparing the average structure of the  $I_{HF}$  ensemble from our simulations to the one experimentally determined. For this purpose we compute the formation probability  $Q_{ij}(Q)$  for each native DHFR contact –involving residues  $(i, j)$ – at different stages of the folding process by averaging the number of times the contact occurs over the set of structures existent in a selected range of  $Q$ . As detailed in Fig. 2, the central result from this analysis is that the main intermediate  $I_{HF}$  is characterized by a largely different degree of formation in different parts of the protein: *domain 1* (i.e. interactions among strands 2-5 and helices 2-3) appears to be formed with probability greater than 0.7 while *domain 2* (i.e. interactions among strands 6-8, helix 1 and helix 4) is almost non existent.

The formation of *domain 1* and *domain 2* during the folding event is more closely understood from Fig. 3 (panels (a) and (c)), where the RMS distance of the parts of the protein constituting each *domain* from the corresponding native structures is shown for a typical folding simulation. Indeed the two *domains* fold in a noticeably different way: in the stable intermediate  $I_{HF}$ , *domain 1* is closer than 5 Å (RMS) to that found in the native structure while *domain 2* is highly variable (RMS distance greater than 15 Å from its native structure). Still, in agreement with hydrogen exchange studies (20), some protection is expected across domains from our simulations and complete protection from exchange is expected only after the formation of the fully folded protein. A combination of fluorescence, CD mutagenic and new drug binding studies on DHFR indeed demonstrate that *domain 1* is largely folded with specific tertiary contacts formed and that this collection of intermediates is obligatory in the folding route (24).

### B. Interleukin-1 $\beta$

Supported by some recent experiments, Heidary et al (25) have proposed a kinetic mechanism for the folding of IL-1 $\beta$  that requires the presence of a well defined on-pathway intermediate species. The structural details of these species were determined from NMR and hydrogen exchange techniques (25,26). We have compared these experimental data with our simulations for the IL-1 $\beta$  G $\alpha$ -like analogue ( Fig. 1 (b) and (d)). The folding picture emerging from these numerical studies differs substantially from that observed for DHFR (see panels (a) and (c) of Fig. 1). An intermediate state is populated for  $Q$  around 0.55, followed by a rate limiting barrier (around  $Q = 0.7$ ) after which the system proceeds to the well defined native state.

Is the theoretical intermediate similar to the one observed experimentally? Using the same procedure employed for the DHFR, a comparison between the average

structure of the IL-1 $\beta$  intermediate ensemble and the one emerging from experimental studies is shown in Fig. 4. These results indicate that the calculated intermediate has residues 40-105 (strands 4-8) folded into a native-like topology but with interactions between strands 5 and 8 not fully completed. Experimental results confirm that strands 6-8 are well folded in the intermediate state and that strands 4-5 are partially formed. However results of experiments and theory differ in the region between residues 110-125 where hydrogen exchange shows early protection and theory predicts late contact formation. This region contains 4 aromatic groups PHE 112, PHE 117, TYR 120, TRP 121 which may be sequestered from solvent due to clustering of these residues and from removal from unfavorable solvent interactions. This effect would not be fully accounted for our model, where all native interactions are considered as energetically equivalent and large stabilizing interactions are not differentiated. Thus, energetics may favor early formation of the structure corresponding to residues 105-125 while topology considerations favor the formation of strands 4-8.

## IV. CONCLUSIONS

Theoretical and experimental studies of protein folding at times appear to be at odds. Theoretical analysis of simple model systems oftentimes predict a large number of routes to the native protein whereas experimental work on larger systems indicates that folding proceeds through a limited number of intermediate species. Although in the eyes of some people these two descriptions are inconsistent with each other, this is clearly not true. The large number of routes may or may not lead to the production of on-route kinetic intermediate ensembles depending on the result of the competition between configurational entropy and the effective folding energy. In this study, we show that productive intermediate species are produced by using simplified protein models, with funnel-like landscapes, based on purely topological considerations and the results are in good agreement with the available experimental data. The fact that these simplified minimally frustrated models for DHFR and IL-1 $\beta$  can predict the overall features of the folding intermediates and transition states experimentally measured for these two proteins, with completely different folding mechanisms and functions, support our general picture that real proteins have a substantially reduced level of energetic frustration and a large component of the observed heterogeneity during the folding event is topologically determined. Such observations lead us to propose that the success in designing sequences that fold to a particular shape is constrained by topological effects. What is more challenging are the consequences of this conclusion — are these topological constraints something that only have to be tolerated during the folding event or are they actually used by biology towards helping function? Here we

speculate only in the context of these two examples, but this question really should be addressed more generally in the future.

## V. ACKNOWLEDGMENTS

This work has been supported by the NSF (Grant # 96-03839), the La Jolla Interfaces in Science program (sponsored by the Burroughs Wellcome Fund), and the NIH (grant # 6M54038). We warmly thank Angel García for many fruitful discussions. One of us (C.C.) expresses her gratitude to Giovanni Fossati for his suggestions and helpful discussions.

1. Leopold, P. E, Montal, M, & Onuchic, J. N. (1992) *Proc. Natl Acad. Sci. USA* **89**, 8721–8725.
2. Onuchic, J. N, Luthey-Schulten, Z, & Wolynes, P. G. (1997) *Annu. Rev. Phys. Chem.* **48**, 545–600.
3. Dill, K. A & Chan, H. S. (1997) *Nature Struct. Biol.* **4**, 10–19.
4. Nymeyer, H, García, A. E, & Onuchic, J. N. (1998) *Proc. Natl Acad. Sci. USA* **95**, 5921–5928.
5. Klimov, D. K & Thirumalai, D. (1996) *Proteins: Struct. Funct. Genet.* **26**, 411–441.
6. Mirny, L. A, Abkevich, V, & Shakhnovich, E. I. (1996) *Folding & Design* **1**, 103–116.
7. Shea, J. E, Nochomovitz, Y. D, Guo, Z. Y, & Brooks, C. L. (1998) *J. Chem. Phys.* **109**, 2895–2903.
8. Li, H, Helling, R, Tang, C, & Wingreen, N. (1996) *Science* **273**, 666–669.
9. Nelson, E. D & Onuchic, J. N. (1998) *Proc. Natl Acad. Sci. USA* **95**, 10682–10686.
10. Nymeyer, H, Socci, N, & Onuchic, J. (1999) *Proc. Natl. Acad. Sci. USA* **97**, 634–639.
11. Onuchic, J, Nymeyer, H, García, A, Chahine, J, & Socci, N. (2000) *Adv. Protein Chem.* in press.
12. Shea, J, Onuchic, J, & Brooks III, C. (1999) *Proc. Natl. Acad. Sci. USA* **96**, 12512–12517.
13. Clementi, C, Nymeyer, H, & Onuchic, J. (2000) *J. Mol. Biol.* in press.
14. Ueda, Y, Taketomi, H, & Gō, N. (1975) *Int. J. Peptide Res.* **7**, 445–459.
15. Ueda, Y, Taketomi, H, & Gō, N. (1978) *Biopolymers* **17**, 1531–1548.
16. Sobolev, V, Wade, R, Vriend, G, & Edelman, M. (1996) *Proteins* **25**, 120–129.
17. Swendsen, R. H. (1993) *Physica A* **194**, 53–62.
18. Onuchic, J, Socci, N, Luthey-Schulten, Z, & Wolynes, P. (1996) *Folding & Design* **1**, 441–450.
19. Jennings, P. A, Finn, B. E, Jones, B. E, & Matthews, C. R. (1993) *Biochemistry* **32**, 3783–3789.
20. Jones, B & Matthews, C. (1995) *Protein Science* **4**, 167–177.
21. Jones, B, Jennings, P, Pierre, R, & Matthews, C. (1994) *Biochemistry* **33**, 15250–15258.
22. Kuwajima, K, Garvey, E, Finn, B, Matthews, C, & Sugai, S. (1991) *Biochemistry* **30**, 7693–7703.
23. Jones, B, Beechem, J, & Matthews, C. (1995) *Biochemistry* **34**, 1867–1877.
24. Heidary, D, O’Neil, J, Roy, M, & Jennings, P. (2000) *Proc. Natl. Acad. Sci. USA* in press.
25. Heidary, D, Gross, L, Roy, M, & Jennings, P. (1997) *Nature Struct Biol* **4**, 725–731.
26. Varley, P, Gronenborn, A. M, Christensen, H, Wingfield, P. T, Pain, R. H, & Clore, G. M. (1993) *Science* **260**, 1110–1113.
27. Plotkin, S & Onuchic, J. (2000) *Proc. Natl. Acad. Sci. USA*. submitted.

# FIGURE CAPTIONS

**Fig. 1 (a)** RMS distances between the DHFR native structure and several computationally determined structures at different values of the reaction coordinate  $Q$  for an unfolding simulation at a temperature slightly above the folding temperature ( $T = 1.01T_f$ ) and **(c)** free energy  $F(Q)$  of the DHFR Gō-like model as a function of  $Q$  around the folding temperature. The folding temperature  $T_f$  is estimated as the temperature where a sharp peak appears in the specific heat plotted as a function of the temperature (data not shown). Both temperatures and free energies are presented in units of  $T_f$ . Notice that the thermal fluctuations around the lowest energy state (i.e.  $Q = 1$ , by construction of the model) account for motions around the free energy minimum. Therefore, the folded state ensemble has a minimum close to  $Q = 1$ , at  $Q \sim 0.9$ , but not exactly at  $Q = 1$ . Indeed at  $Q = 1$  the structure would be frozen in the native configuration. A similar remark applies for the IL-1 $\beta$  free energy profile shown in panel (c). The energy of a configuration, as quantified by the color scale on the top of the figure, is here defined as the bare value of the effective potential function in that configuration (i.e. no configurational entropy is accounted in the energy). Differences between energy and free energy (at finite temperature) are due to the configurational entropy contribution to the free energy. In panel (c) a main intermediate ensemble  $I_{HF}$  emerges in the folding process as a local minimum at  $Q$  around 0.4 after the overcoming of the first barrier. Indeed this local minimum corresponds to a populated region in panel (a) (after the scarcely populated barrier around  $Q = 0.3$ ) with energy significantly lower than in the unfolded state. This main intermediate then evolves toward a set of structures close to the native states (located between  $Q = 0.7$  and  $Q = 0.8$ ) that eventually interconvert into the fully folded state. A transient set of structures, close to the native state, is also apparent from Fig. 3 (b). The folding scheme resulting from these simulations is consistent with the sketch of Fig. 3 (d), proposed from the experimental data (19,24).

**(b)** RMS distances between the native structure and several computationally determined structures at different values of the reaction coordinate  $Q$  for a folding simulation of the Gō-like model of IL-1 $\beta$ . The simulation is performed at a temperature near to the folding temperature ( $T = 0.99T_f$ ). **(d)** Free energy  $F(Q)$  as a function of  $Q$  around to the folding temperature. The folding temperature is estimated from the sharp peak in the specific heat curve as a function of the temperature (data not shown). An intermediate ensemble is populated during the folding event and it is identified by the broad local minimum in the free energy profile (around  $Q = 0.55$ ), and the corresponding populated region in panel (b) (with energy significantly lower than in the unfolded state). These results are consistent with the kinetic mechanism for the folding of IL-1 $\beta$  proposed by Heidary et al. (25). A set of structures close to the native conformation is transiently populated for  $Q$  between

0.75 and 0.8 (see panel (b) and the corresponding “flat” region in the free energy panel (d)). This fact could be interpreted as the presence of an additional intermediate state close to the native state. Experimentally the possibility that another partially unfolded form could be populated during the folding process is currently under investigation. Several constant temperature simulations (both folding and unfolding simulations) of the two protein models were made and combined to generate the free energy plots.

**Fig. 2** The probability  $Q_{ij}(Q)$  of the native DHFR contacts to be formed, as resulting from the simulations at different stages of the folding process: **(a)** at an early stage ( $Q = 0.1 \pm 0.05$ ), **(b)** at the main intermediate – located in the interval  $Q = 0.4 \pm 0.05$  (see panels (a) and (c) of Fig. 1) and **(c)** at a late stage of the folding process ( $Q = 0.7 \pm 0.05$ ). In an topologically and energetically perfectly smooth funnel-like energy landscape, at any value  $Q$  during the folding, any contact  $(i, j)$  should have a probability  $Q_{ij}(Q)$  to be formed equal to  $Q$  (2). By computing  $Q_{ij}(Q)$  for each contact over different windows of the reaction coordinate  $Q$ , we can quantify the deviations from this smooth funnel behavior and locate the early and late contacts along the folding process. It is worth noticing that any deviation from the “perfectly smooth” behavior is mainly due to topological constraints, since energetic frustration has been mostly removed from the system. Different colors in the contact maps indicate different probability values from 0 to 1, as quantified by the color scale at the top. The preference to form more local structure than non-local in the almost unfolded state (b) is due to the smaller conformational entropy loss by forming local contacts than by pinching off longer loops (27). The most interesting result is that *domain 1*, identified by the interactions among strands 2-5 and helices 2-3, is substantially formed at the intermediate  $I_{HF}$  (probabilities for individual contacts greater than 0.7), while the formation of *domain 2* (i.e. interactions among strand 1, strands 6-8, helix 1 and helix 4) is highly unfolded (contact probabilities between 0 and 0.4). Helix 1 and helix 4 are largely formed, but their interactions with the remainder of the proteins are loose (probabilities less than 0.4). Overall, this description of the structure of the main intermediate  $I_{HF}$  – *domain 1* almost formed and *domain 2* largely unformed – is in agreement with the structure of  $I_{HF}$  experimentally observed. Moreover, the latest events in the folding process (panel (c)) appear to be the formation of interactions between strands 7-8 and the remainder of the protein. This again has been experimentally determined. Panel **(d)** illustrates the regions of the native structure that simulations and experiments agree to indicate as formed at the intermediate  $I_{HF}$ .

**Fig. 3** The RMS distances between the regions of the DHFR structure identified as **(a)** *domain 1* and **(c)** *domain 2* and their corresponding native configurations are plotted versus the reaction coordinate  $Q$ . *Domain 1* collapses to a structure close to its native conformation (RMS distance less than 5 Å) in the early stages of folding, leading to the formation of the main intermediate  $I_{HF}$  (located at  $Q$  around 0.4) whereas *domain 2* remains largely unfolded (RMS distance larger than 15 Å). In the interval of  $Q$  from 0.6 to 0.8 there are several possible structures. Consistently with the multi-channel folding model proposed from experimental evidences (19), from panels (a) and (c) one can propound several possible ways to proceed from  $I_{HF}$  to the folded state. In panel **(b)** the fraction of native contacts formed,  $Q$ , is plotted versus the simulation time for a region of our simulations where the transition from folded to unfolded state is observed (at a simulation temperature slightly higher than the folding temperature,  $T = 1.01T_f$ ). A set of structures close to the native state ( $Q$  around 0.7) is transiently populated. Different colors represent different energies of a configuration (quantified by the top energy scale), as well as for panels (a) and (c). **(d)** The kinetics mechanism for the folding of DHFR, proposed on the basis of experimental results (19–24). Experimentally a first step of folding is detected as a very rapid collapse of the unfolded form to the burst-phase intermediate ( $I_{BP}$ ) which has a significant content of secondary structure. The folding state is reached through four different channel, involving the formations of the main intermediate  $I_{HF}$ .  $I_{HF}$  is represented as a set of structures  $I_1 - I_4$  structurally similar to each other but proceeding towards the native state with a different rate. These intermediate structures evolve to the native forms  $N_1 - N_4$  via slow-folding reactions.

(d). The small difference between simulations and experiments (contact formation in the region between residues 110-125) may be due to energetic considerations that are not taken into account in the model, as discussed in the text. In agreement with experimental results, the formation of contacts between N and C terminus is not accomplished until the late stage of folding – these contacts are still unformed for  $Q = (0.6 - 0.7)$  (data not shown).

**Fig. 4** Probability of the contact formation for the native contacts, as obtained during a typical folding simulation (data shown are obtained at  $T = 0.99T_f$ ) of the IL-1 $\beta$  at different stages of the folding: **(a)** in a range of  $Q$  between 0.3 and 0.4 that corresponds to the early stage of folding leading to the formation of the intermediate ensemble; and **(b)** at the intermediate ( $Q$  between 0.45 and 0.55). At the intermediate the interactions involving strands from 4 to 8 are almost completely formed; interactions among strands 1-3 are likely formed but interactions between them and the rest of the protein are loose. Contacts involving strands 9-12 appear weakened and the interactions between N (residues 1-40) and C terminus (residues 110-153) are completely unformed. Experimental results confirm that strands 6-8 are well folded in the intermediate state and that strands 4-5 are partially formed. Panels **(c)** and **(d)** show the regions of the IL-1 $\beta$  native structure formed at the intermediate, as resulting from simulations (c) and experiments

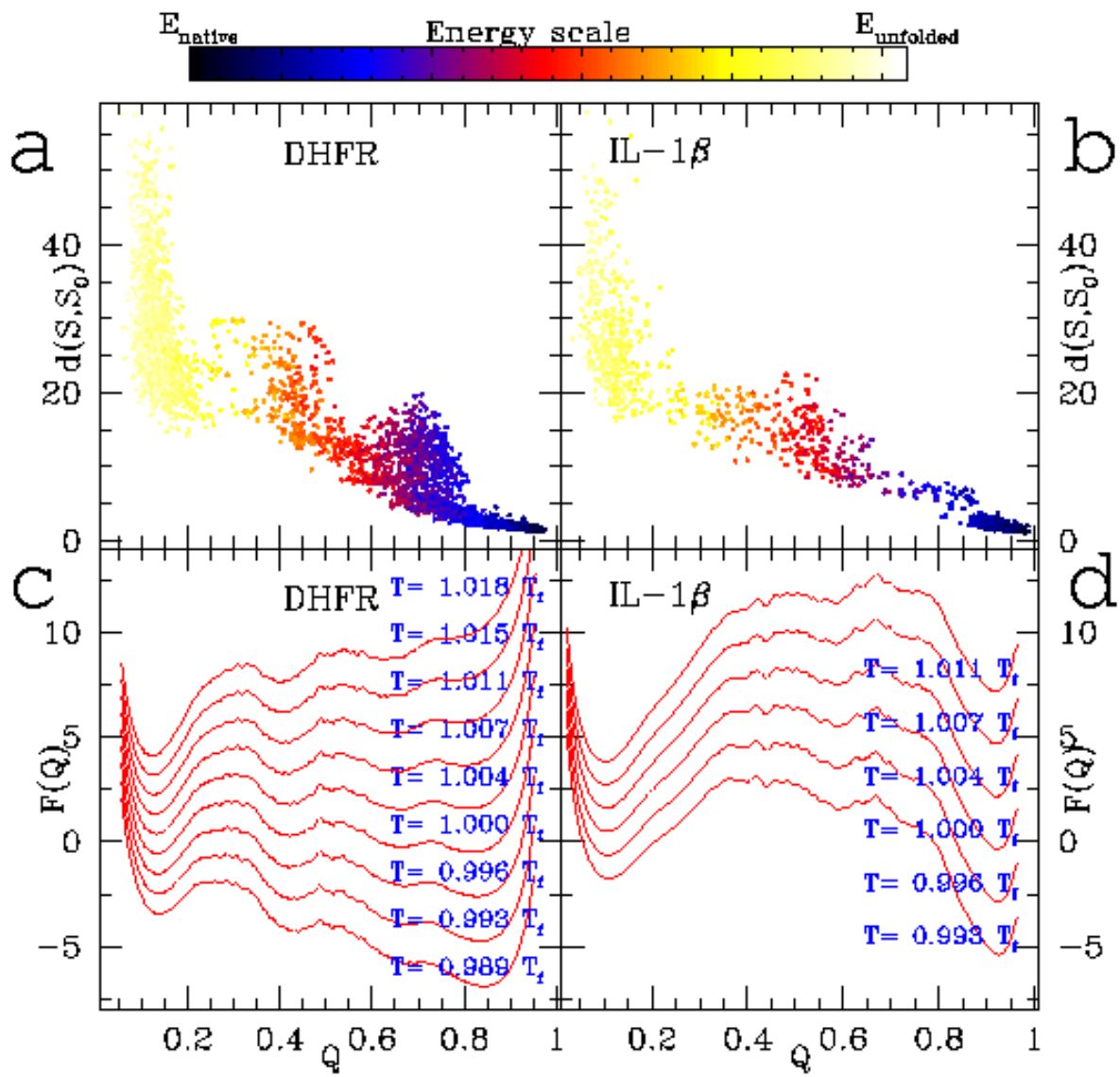


FIG. 1.



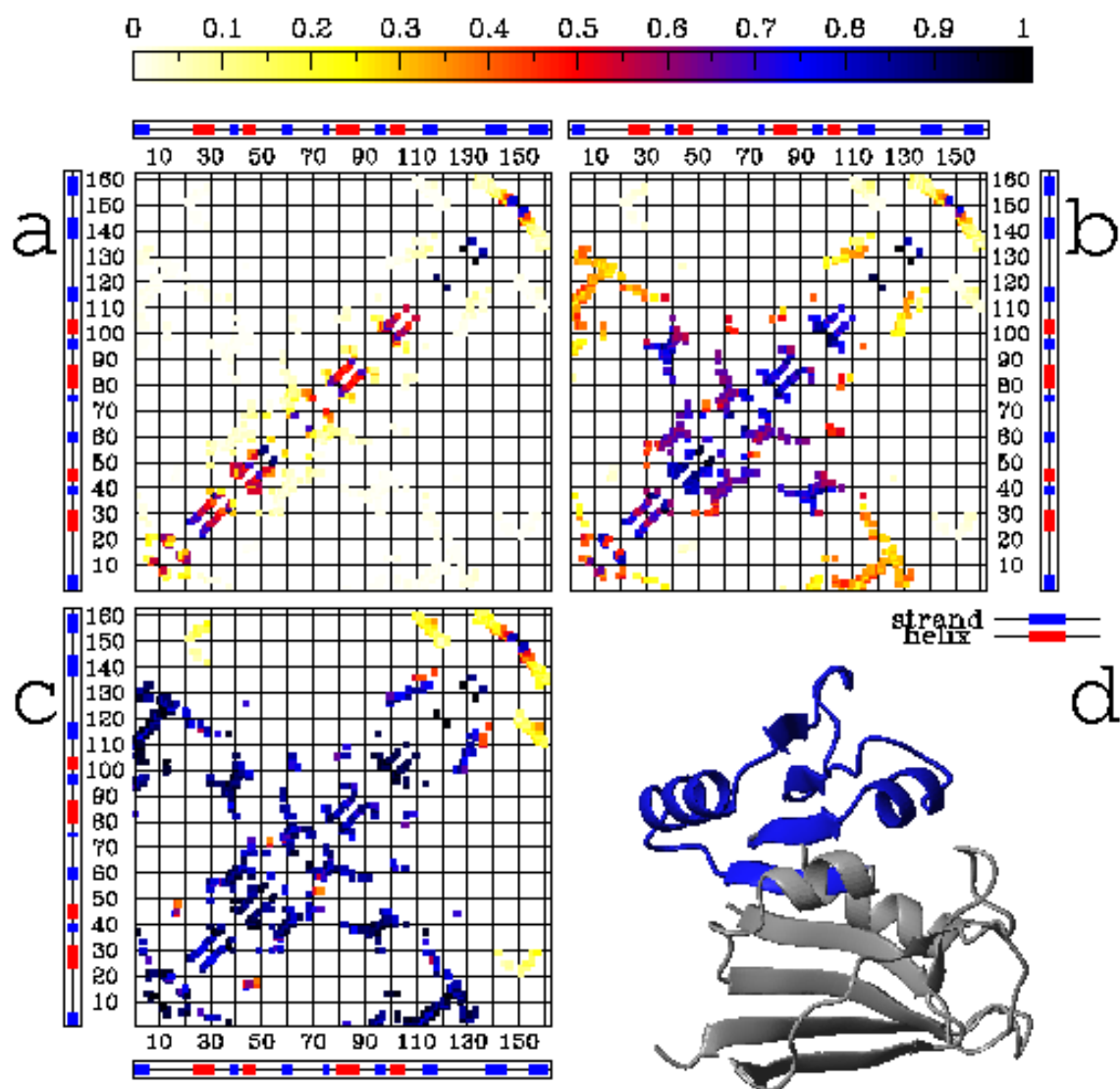


FIG. 2.

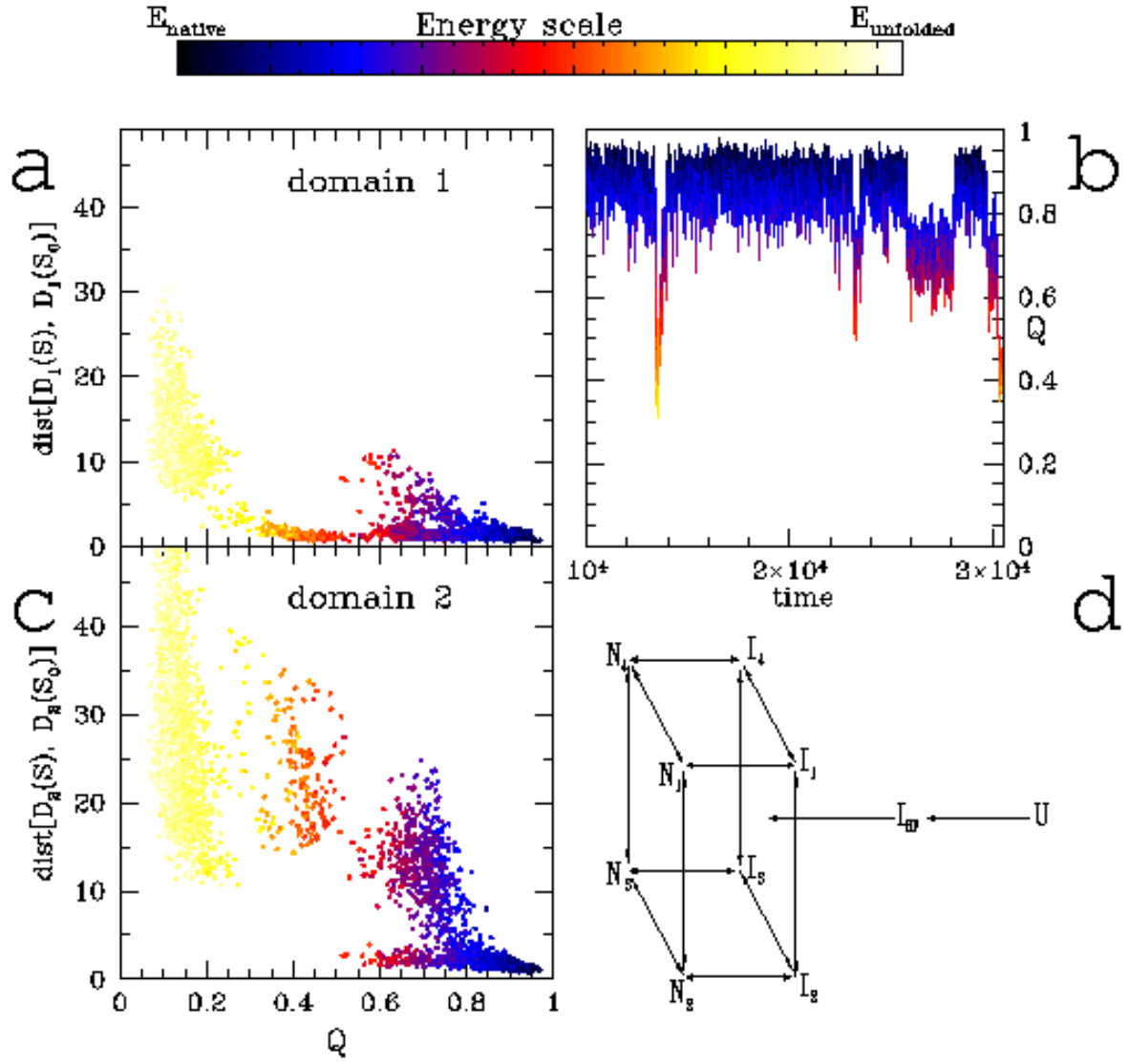


FIG. 3.

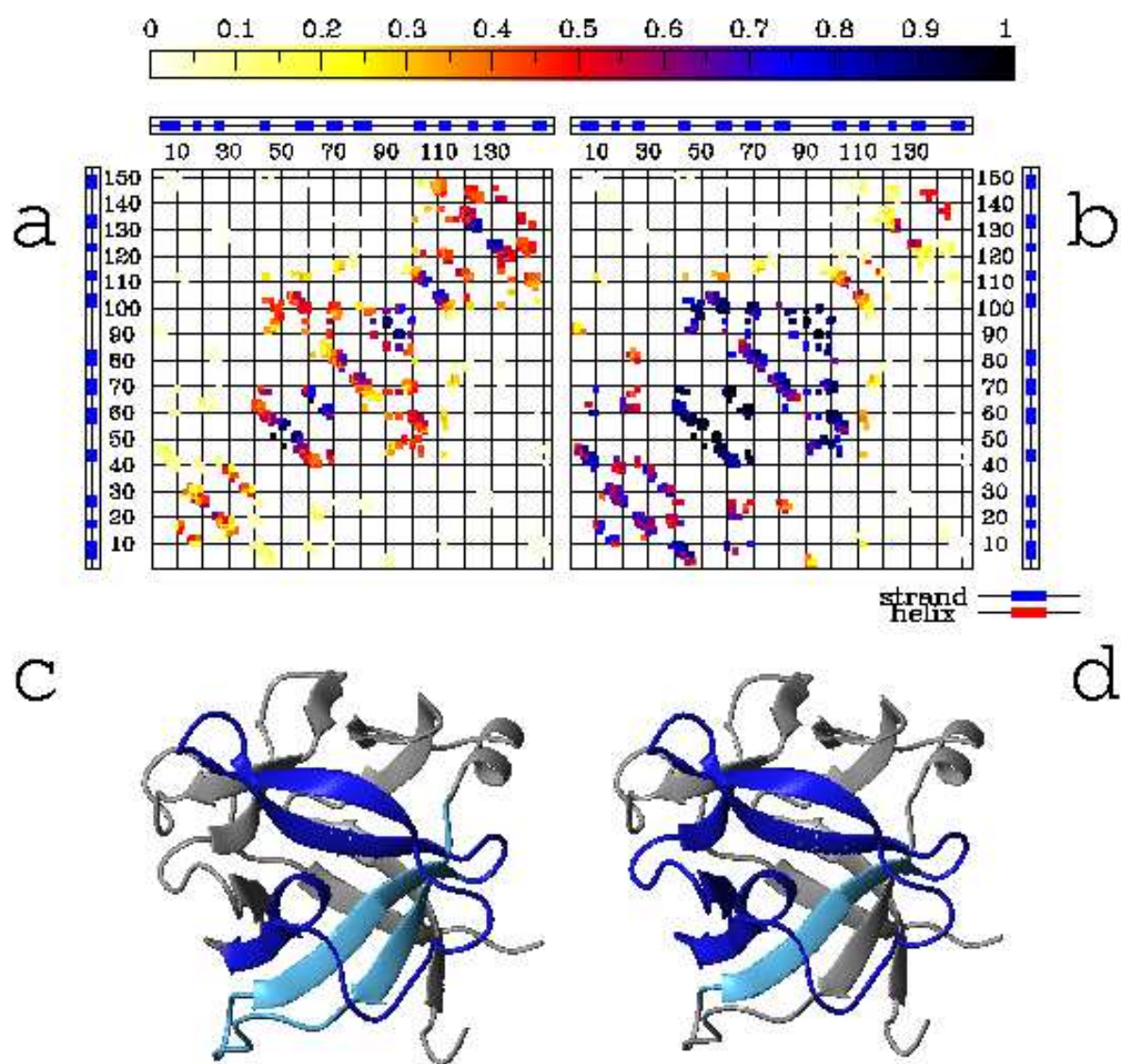


FIG. 4.